Aggregated neutrophil extracellular traps limit inflammation by degrading cytokines and chemokines

Christine Schauer[1], Christina Janko[1,2], Luis E Munoz[1], Yi Zhao[1,3], Deborah Kienhöfer[1], Benjamin Frey[4], Michael Lell[5], Bernhard Manger[1], Jürgen Rech[1], Elisabeth Naschberger[6], Rikard Holmdahl[7], Veit Krenn[8], Thomas Harrer[1], Ivica Jeremic[1,9], Rostyslav Bilyy[10], Georg Schett[1], Markus Hoffmann[1] & Martin Herrmann[1]

Gout is characterized by an acute inflammatory reaction and the accumulation of neutrophils in response to monosodium urate (MSU) crystals. Inflammation resolves spontaneously within a few days, although MSU crystals can still be detected in the synovial fluid and affected tissues. Here we report that neutrophils recruited to sites of inflammation undergo oxidative burst and form neutrophil extracellular traps (NETs). Under high neutrophil densities, these NETs aggregate and degrade cytokines and chemokines via serine proteases. Tophi, the pathognomonic structures of chronic gout, share characteristics with aggregated NETs, and MSU crystals can induce NETosis and aggregation of NETs. In individuals with impaired NETosis, MSU crystals induce uncontrolled production of inflammatory mediators from neutrophils and persistent inflammation. Furthermore, in models of neutrophilic inflammation, NETosis-deficient mice develop exacerbated and chronic disease that can be reduced by adoptive transfer of aggregated NETs. These findings suggest that aggregated NETs promote the resolution of neutrophilic inflammation by degrading cytokines and chemokines and disrupting neutrophil recruitment and activation.

The ejection of chromatin into the extracellular space during the formation of NETs has been described as a proinflammatory response of neutrophils to immobilize and kill extracellular pathogens[1–3]. Formation of NETs is enhanced by reactive oxygen species (ROS) produced from cells undergoing an oxidative burst[4,5]. In particular, ROS were shown to be important for the release of proteases that mediate disruption of membranes at later stages of NETosis[6,7]. Aside from containing chromatin, NETs also contain bactericidal molecules and enzymes from neutrophil granules. In addition, NETting neutrophils release a variety of proinflammatory mediators that orchestrate the local innate immune response.

Similarly to microorganisms, MSU crystals act as danger signals that induce proinflammatory responses. Over the course of evolution, humans have lost the enzymatic activity of uricase and therefore display elevated levels of the strong antioxidant uric acid[8] that has a maximal limited solubility in aqueous solution of about $600\,\mu M$[9,10]. In individuals with hyperuricemia, uric acid precipitates in the sodium-rich extracellular milieu as MSU crystals that can induce renal calculi and gouty arthritis. Uptake of MSU crystals by macrophages leads to activation of the NALP3 (also called NLRP3) inflammasome, secretion of the proinflammatory cytokines interleukin-1β (IL-1β) and IL-18 and recruitment of neutrophils[11,12]. Neutrophils

also ingest MSU crystals and respond initially by releasing inflammatory mediators, including tumor necrosis factor-α (TNF-α) and IL-6, as well as neutrophil attractants (for example, IL-8) and activators (for example, MIP-1α (also called CCL3) and IP-10 (also called CSCL10))[13–15]. To avoid a positive feedback loop of cell activation and mediator release, stringent control of these processes is required. As such, acute inflammatory attacks and pain in gout often resolve within a few days, although MSU crystals can still be detected in the synovial fluid[16] and affected tissues. The mechanisms mediating rapid control and termination of MSU-triggered inflammation remain unclear.

In advanced disease, the MSU crystals are embedded in an amorphous whitish matrix referred to as a tophus. These tophi are localized macroscopic lesions that can be clinically silent for a long time, suggesting that a certain containment of inflammation takes place.

In this study, we show that gouty tophi are composed of extended areas of extracellular DNA colocalizing with material from neutrophil granules, such as neutrophil elastase (NE), myeloperoxidase or cathelicidins. Such colocalization is typical for neutrophils that have undergone NETosis[1,17].

At low neutrophil cell densities, MSU crystals induced ROS-dependent NET formation accompanied by cytokine and chemokine release. In contrast, following neutrophil recruitment, when neutrophils are at

[1]Department of Internal Medicine 3, University of Erlangen-Nuremberg, Erlangen, Germany. [2]Department of Otorhinolaryngology, Head and Neck Surgery, Section for Experimental Oncology and Nanomedicine (SEON), University Hospital Erlangen, Erlangen, Germany. [3]Department of Rheumatology and Immunology, West China Hospital, Sichuan University, Chengdu, China. [4]Department of Radiation Oncology, University Hospital Erlangen, Erlangen, Germany. [5]Department of Radiology, Friedrich-Alexander University of Erlangen-Nuremberg, Erlangen, Germany. [6]Division of Molecular and Experimental Surgery, Department of Surgery, University of Erlangen Medical Center, Erlangen, Germany. [7]Division of Medical Inflammation Research, Department of Medical Biochemistry and Biophysics, Karolinska Institute, Stockholm, Sweden. [8]Department of Pathology, MVZ of Pathology, Trier, Germany. [9]Institute of Rheumatology, School of Medicine, University of Belgrade, Belgrade, Serbia. [10]Institute of Cell Biology, National Academy of Sciences of Ukraine, Lviv, Ukraine. Correspondence should be addressed to M.H. (markus.hoffmann@uk-erlangen.de).

Figure 1 Characterization of MSU-induced NETs in tophi and synovial fluid from subjects with gout. (**a**) DECT scans and corresponding photographs of the hand of gout case 73,423 during acute highly inflammatory gout and during a chronic intercritical phase. Deposits of urate are shown in green, and deposits of calcium are shown in purple. A control scan and corresponding picture of a subject (case 14,572) suffering from gout in the feet but not the hands is also shown. (**b**) Representative tissue sections from an individual with gout, including a tophus, and from a subject with non-gouty synovitis stained with PI and an antibody to NE. White arrows indicate areas where extranuclear DNA and NE colocalize in the tophus area. Control stains were performed with PI and secondary FITC-conjugated antibody only. Scale bars, 200 μm. (**c**) Quantitative analysis of the fluorescence intensity and maximal connected PI-positive area in patients with tophaceous gout and MSU-free synovitis. (**d**) Representative immunofluorescence images of DAPI- and NE-stained cytospins from synovial fluid of patients with gout (containing MSU crystals) and MSU-free arthritis (rheumatoid arthritis). White arrows show spread NETs in gout samples, and blue arrows indicate diffused NETs. The images in the upper right corners show a higher magnification of a diffused NET and a regular synovial neutrophil. Scale bars, 100 μm.

(**e**) Quantification of nuclear morphology in synovial fluid samples from patients with gout and MSU-negative arthritis (rheumatoid arthritis). Bars show the mean ± s.e.m. of the percentage of cells exhibiting morphology of cells with regular nuclei (No NETs), diffused (Diff.) and spread (Spr.) NETs. *$P < 0.05$ as determined by Mann-Whitney U test ($n = 4$).
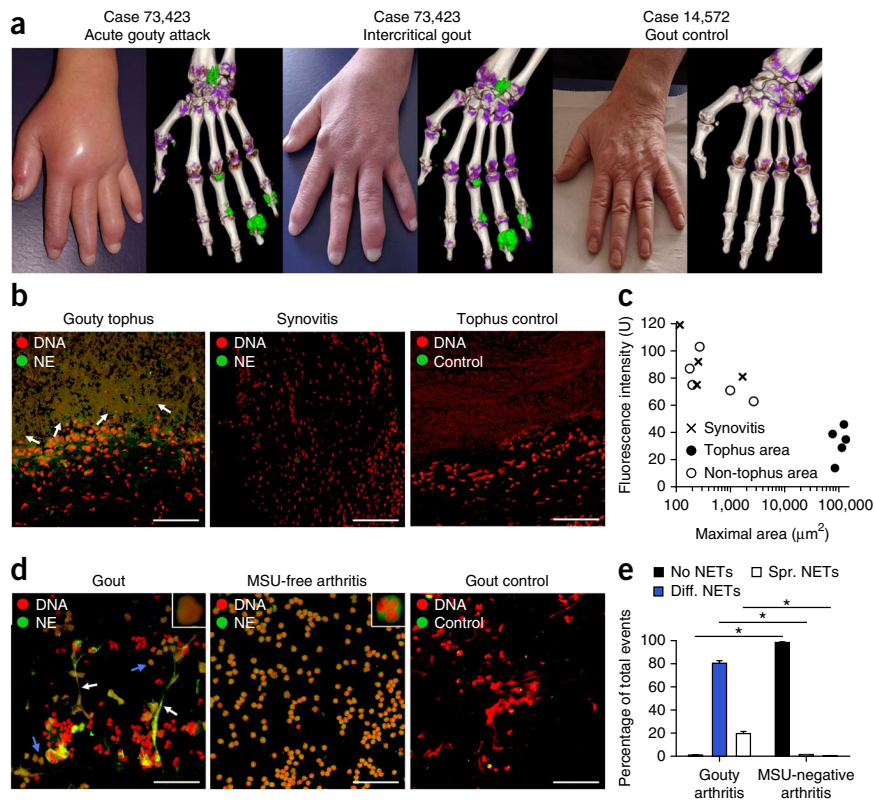
high cell densities similar to those occurring in inflamed tissue, MSU-induced NETs formed dense aggregates resembling gouty tophi that sequester and degrade neutrophil inflammatory mediators. In support of this observation, mice that cannot form aggregated NETs (aggNETs) because of an inability to produce ROS from phagocytes develop chronic and exacerbated neutrophil-driven paw inflammation in response to MSU crystals or the Toll-like receptor 2 (TLR2) agonist zymosan that can be ameliorated by adoptive transfer of aggNETs. Higher production of neutrophil-derived chemokines was also apparent in wild-type mice when aggregation of NETs was inhibited with DNase I. These data suggest that complex aggNET structures promote the resolution of neutrophil-induced inflammation by trapping and degrading proinflammatory mediators.

RESULTS
Gouty tophi share characteristics with NETs

Clinically overt gouty tophi and subclinical urate deposits in humans can be detected by dual energy computed tomography (DECT)[18,19] In DECT images of individuals with gout, we noticed that deposits of urate detected during a highly inflammatory phase persisted during a clinically silent (intercritical gout) phase (**Fig. 1a**).

Next we analyzed whether NETs, extranuclear DNA structures colocalizing with material from neutrophil granules, can be found in human tissue sections of subjects with gout and control individuals. Extranuclear DNA colocalizing with NE was abundant in the tophus, whereas in the non-tophus area and in MSU-negative synovitis, neutrophils were sparse, and the DNA exhibited a predominantly nuclear appearance (**Fig. 1b**). Quantification of the area covered by propidium iodide (PI)-positive material and of the fluorescence intensity of the

PI signal indicated large stretches of diluted extracellular DNA spread over the tophus as compared to a more regular nuclear morphology in the adjacent tissue and in non-gouty synovitis (**Fig. 1c**). We analyzed cytospins from synovial fluid obtained from individuals with gout and MSU-negative arthritis and detected extracellular thready chromatin colocalizing with NE only when the synovial fluid contained MSU crystals (**Fig. 1d**). After classifying NETs into diffused and spread NETs as described previously[20], we found a significantly higher number of cells that had undergone NETosis in the samples from gout than in those from MSU-negative arthritis (**Fig. 1e**).

### MSU crystals induce NETosis and aggregation of NETs

Our observations from subjects with gout prompted us to further examine whether MSU crystals can induce NETosis. When analyzing the *in vitro* interaction of DNA-stained human neutrophils with MSU crystals by video microscopy, we observed rearrangement of the neutrophils' nuclear structures followed by rapid cellular disintegration that was independent of phagocytosis of the crystals (**Supplementary Videos 1** and **2**). During this disintegration process, chromatin was externalized, forming NETs comparable to those induced by microorganisms and cytokines[21].

Inflamed tissues are characterized by dense infiltration of neutrophils. To mimic the situation during acute inflammation *in vivo*, we increased the density of neutrophils in our *in vitro* NETosis assays to values typically encountered in the synovial fluid of highly inflamed joints (2×10^7 neutrophils ml^{-1}) or densely infiltrated tissue (10^8 neutrophils ml^{-1})[22]. Under these conditions, MSU crystals induced aggregation of NETs within 10 min (**Fig. 2a**). In cryosections of these aggregates, we found extracellular DNA colocalized with granule

Figure 2 MSU crystals trigger NETosis and aggregation of NETs in cultured human neutrophils. (**a**) Representative polarization microscopy images of isolated human neutrophils cultured in high density (1×10^8 cells ml^{-1}) with MSU crystals with or without various inhibitors. NAC, *N*-acetylcysteine. Scale bars, 50 μm. (**b**) Representative polarization microscopy images of 5×10^6 neutrophils ml^{-1} incubated with MSU crystals and lactoferrin, ATP or BSA. Scale bars, 50 μm. (**c**) Quantitative analysis of the size of aggregates induced in human neutrophils cultured with MSU crystals at high and low densities with or without inhibitors or inducers. Shown are measurements of neutrophils from individual donors and medians (red bars). BHA, butylated hydroxyanisole; DPI, diphenylene iodonium; Asc acid, ascorbic acid. (**d**–**h**) Representative fluorescence microscopy images of MSU-treated (**d**,**g**), untreated (**e**) or Triton-treated (**h**) human neutrophils cultured at different concentrations and stained for DNA (DAPI) and NE. Control staining (**f**) was performed using DAPI and secondary FITC-conjugated antibody only. Scale bars, 100 μm.
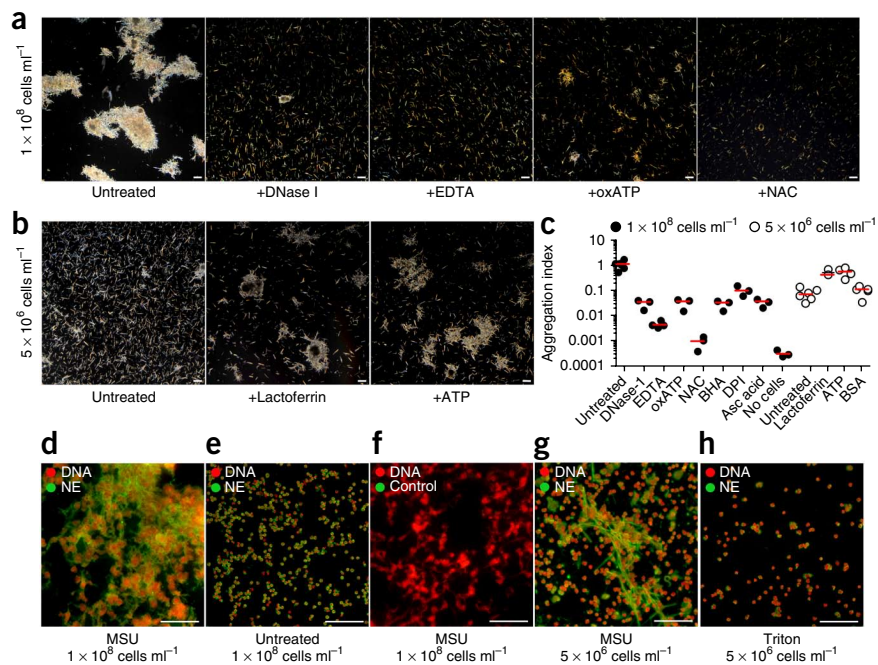
proteins (**Fig. 2d** and **Supplementary Fig. 1**) that resembled gouty tophi. High doses of DNase I, the bivalent cation-chelating agent EDTA, the ATP antagonist oxidized ATP (oxATP) and the ROS inhibitor *N*-acetylcysteine (NAC) inhibited the formation of these aggNETs (**Fig. 2a,c** and **Supplementary Fig. 2**), whereas inhibitors of Rho-associated protein kinase or of tissue transglutaminase had no effect (data not shown). MSU crystals promoted aggregation in a dose-dependent manner and at a concentration as low as 50 μg ml^{-1} (**Supplementary Fig. 3a,b**), suggesting that the aggregation we observed *in vitro* could also occur under physiological conditions in inflamed tissue. In contrast, in low-density cultures (5×10^6 neutrophils ml^{-1}), we observed NETosis but no aggregation of NETs after incubating with MSU (**Fig. 2b** and **Supplementary Fig. 3a,b**). The size of the aggNETs depended on the density of neutrophils in the culture only and was not influenced by the addition of peripheral blood mononuclear cells (**Supplementary Fig. 3c,d**). However, addition of the autocrine neutrophil stimulants ATP or lactoferrin to low-density cell cultures promoted the formation of aggNETs, whereas treatment with BSA as a control had no such effect (**Fig. 2b,c**). MSU-treated but not untreated or Triton-treated (necrotic) neutrophils formed large stretches of extracellular material where DNA and NE colocalized, suggesting the formation of NETs (**Fig. 2d–h**).

Apart from NETosis, necrosis can result in the release of DNA into the extracellular space[23]. However, DNA released during necrosis and other forms of cell death is not normally associated with material from neutrophil granules. To ensure that the changes we observed in MSU-treated neutrophils are due to NETosis, we compared and quantified morphological changes in the nuclei of neutrophils treated with MSU crystals, the TLR2 agonist zymosan and a panel of known inducers of necrosis. Although we observed enlarged nuclei and concomitant lower DAPI fluorescence intensity in necrotic cells, most likely caused by release of DNA into the cytoplasm, we did not detect cloudy or filamentous structures that co-stained with PI and NE, which are typical for NETs (**Fig. 2h** and **Supplementary Fig. 4a**). In contrast, we observed colocalization of DNA and NE indicative of NETs in cells exposed to MSU crystals or zymosan. Furthermore,

quantification of the PI-positive area and the circularity index of PI-positive events allowed us to discriminate between necrotic and NETting cells, as filaments in NETs span a higher perimeter and have a less round shape as compared to extranuclear DNA from necrotic cells (**Supplementary Fig. 4b**).
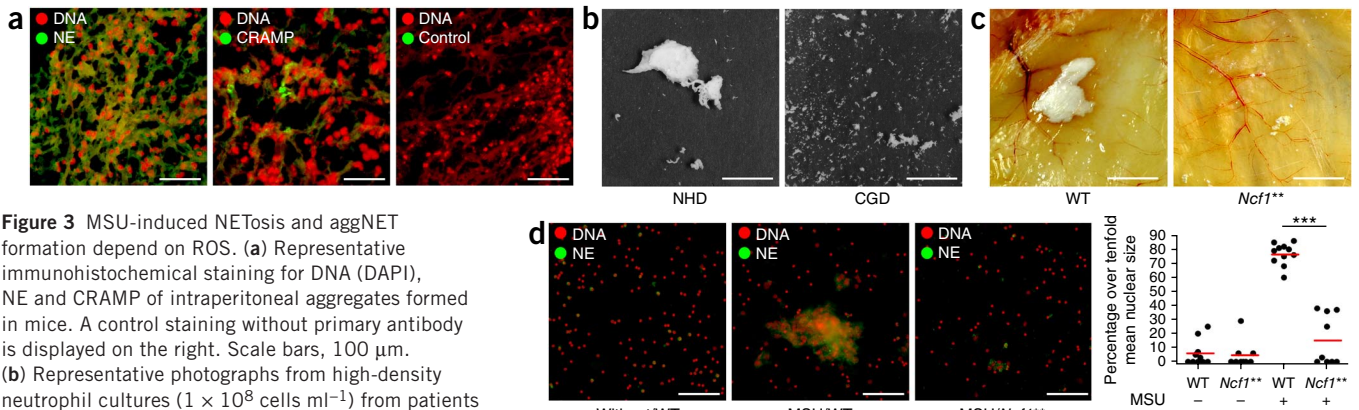
Aggregated NET formation depends on ROS *in vitro* and *in vivo*

The observation of aggNETs elicited by MSU crystals in high-density neutrophil cultures prompted us to explore whether such structures are also formed *in vivo*. Intraperitoneal (i.p.) injection of MSU crystals into mice that had been pretreated with thioglycolate to induce accumulation of neutrophils in the peritoneum resulted in the formation of peritoneal aggregates of amorphous material clumped together in pale whitish clots. Similar to the tophous structures in human subjects with gout[19], these structures in mice can be visualized by DECT (**Supplementary Fig. 5**). Aggregates contained high numbers of MSU crystals, as well as NET-like structures composed of extranuclear DNA colocalizing with NE or cathelicidin-related antimicrobial peptide (CRAMP) (**Fig. 3a**).

Neutrophils from individuals carrying mutations in subunits of the phagocyte NADPH oxidase complex (NOX2) cannot mount an oxidative burst. As a consequence, they suffer from chronic granulomatous disease (CGD) characterized by recurrent bacterial and fungal infections associated with persistent inflammation. As NETosis depends on the production of ROS, individuals with CGD exhibit reduced NETosis[4,5]. The formation of aggNETs was reduced in neutrophils isolated from subjects with CGD and cultured in high cell densities with MSU crystals (**Fig. 3b** and **Supplementary Fig. 6a**).

*Ncf1*** mice carry a single mutation in neutrophil cytosolic factor 1 (encoded by *Ncf1*), a regulatory subunit of the Nox2 complex, that completely abrogates production of ROS by Nox2 (refs. 24,25) and can be considered a model of CGD. To analyze NET formation *in vivo*, we injected MSU crystals into air pouches of wild-type (WT) and *Ncf1*** mice as described previously[12]. In accordance with our results from subjects with CGD, NET aggregation was reduced in air pouches from *Ncf1*** mice (**Fig. 3c** and **Supplementary Fig. 6b**). The observed

Figure 3 MSU-induced NETosis and aggNET formation depend on ROS. (**a**) Representative immunohistochemical staining for DNA (DAPI), NE and CRAMP of intraperitoneal aggregates formed in mice. A control staining without primary antibody is displayed on the right. Scale bars, 100 μm. (**b**) Representative photographs from high-density neutrophil cultures (1×10^8 cells ml^{-1}) from patients with CGD and normal healthy donors (NHD) incubated with MSU crystals for 1 h. Scale bars, 1 cm. (**c**) Representative photographs of aggNETs formed after injection of 5 mg MSU crystals into preformed air pouches on the back of WT and ROS-deficient Ncf1** mice. Scale bars, 1 cm. (**d**) Representative fluorescence microscopy images and quantitative analysis of NETting cells in whole blood drawn from WT mice and oxidative burst–deficient Ncf1** mice incubated with or without MSU crystals, as indicated. Scale bars, 200 μm. Scatter plots show values from individual mice and means (red bars) of percentages of events with over tenfold mean nuclear size. ***$P < 0.001$ as determined by Mann-Whitney U test.

aggNETs in WT mice were characterized by colocalization of DNA and NE (**Supplementary Fig. 6c**). Furthermore, *in vitro* NETosis induced by MSU crystals was reduced in peripheral blood neutrophils from Ncf1** compared to WT mice (**Fig. 3d**).

AggNETs degrade neutrophil-derived inflammatory mediators

Next we analyzed the inflammatory mediators released during MSU-induced NETosis and aggregation of NETs. Whereas cytokines and chemokines were detected at high concentrations in
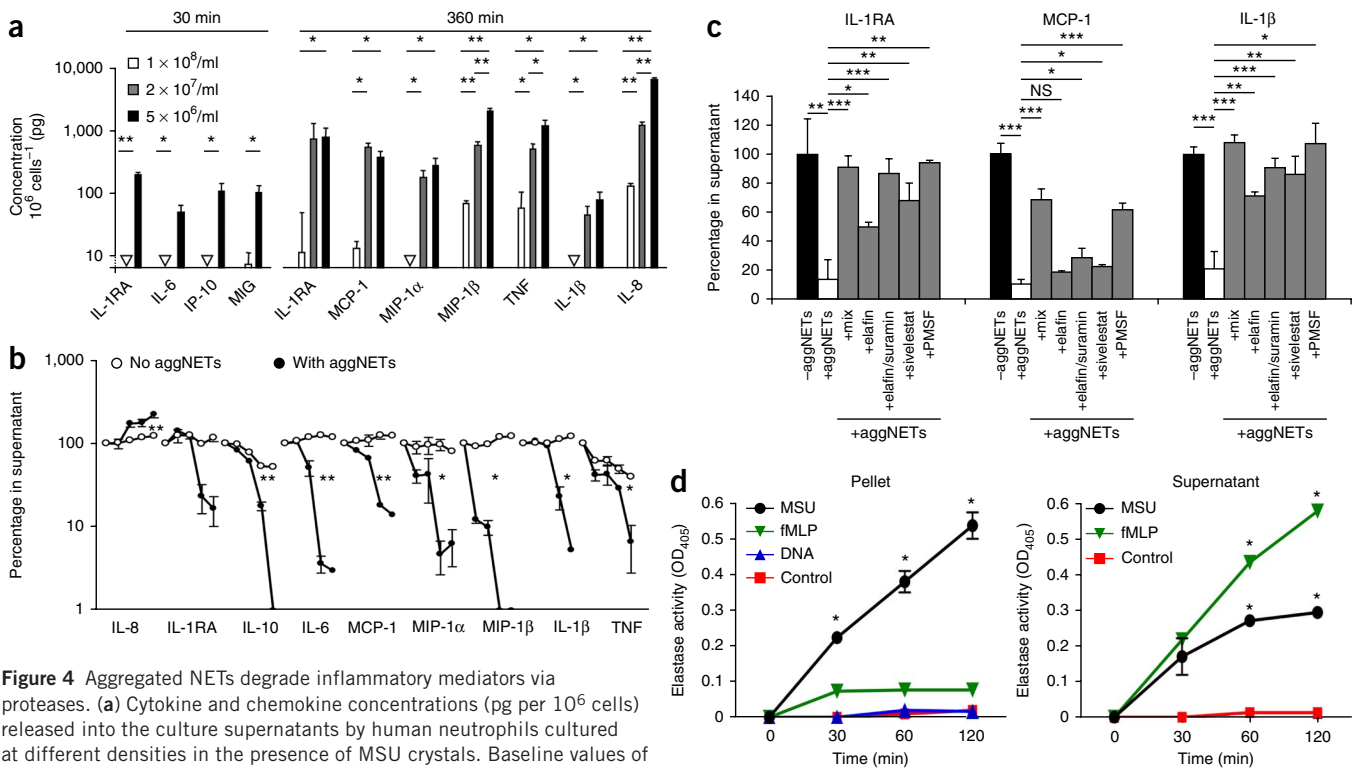
Figure 4 Aggregated NETs degrade inflammatory mediators via proteases. (**a**) Cytokine and chemokine concentrations (pg per 10^6 cells) released into the culture supernatants by human neutrophils cultured at different densities in the presence of MSU crystals. Baseline values of mock-treated neutrophils are subtracted. ∇ indicates a value below the detection limit. Bars show the means ± s.d. of triplicates in one representative experiment out of three total experiments. (**b**) Time course of the degradation of exogenously added cytokines or chemokines by preformed aggNETs. Circles represent the time points 0, 2, 6, 18 and 24 h after co-incubation. Shown are the means ± s.e.m. from three to six donors. *$P < 0.05$, **$P < 0.01$ of areas under the curve as determined by Mann-Whitney U test (**a,b**). (**c**) Inhibition of proteolytic activity of aggNETs by a pan-proteinase inhibitor mix (mix), the proteinase 3 and NE inhibitors elafin and suramin (elafin/suramin), the NE inhibitor sivelestat and the serine proteinase inhibitor PMSF. Bars show the mean ± s.e.m. of the concentrations in supernatants from three independent experiments. *$P < 0.05$, **$P < 0.01$, ***$P < 0.001$ as determined by Student's t test with Dunnett's *post-hoc* test. NS, not significant. (**d**) NE activity in pellets or supernatants of isolated human neutrophils (1×10^8 cells ml^{-1}) incubated with or without MSU crystals, fMLP or purified neutrophil DNA. The plots show the means ± s.e.m. from three independent donors. *$P < 0.05$ as determined by Kruskal-Wallis test ($n = 3$). OD$_{405}$, optical density at 405 nm.

Figure 5 Inability to form NETs results in chronic MSU-induced neutrophilic inflammation. (**a**) Concentrations of inflammatory mediators in the lavage of air pouches of WT and *Ncf1*** mice 24 h after injection of 5 mg MSU crystals with (+) or without (−) preformed aggNETs. The scatter plots show individual measurements and medians of concentrations in lavages of individual mice. **$P < 0.01$ as determined by Student's *t* test with Dunnett's *post-hoc* test. (**b**) Paw edema elicited by subcutaneous injection of MSU crystals into the foot pads of *Ncf1*** and WT mice. The scatter plots show individual measurements and means of the relative thickness of the MSU-injected foot normalized to the contralateral PBS-injected foot. Representative paws of a WT and a *Ncf1*** animal 1 and 46 d after MSU injection are depicted below. ***$P < 0.001$ as determined by Mann-Whitney *U* test. (**c**,**d**) Paw edema induced by subcutaneous injection of zymosan into the foot pad. Shown are individual measurements and means of the relative thickness of the zymosan-injected foot normalized to the contralateral PBS-injected foot. *$P < 0.05$ of areas under the curves as determined by Mann-Whitney *U* test. (**c**) Modulation of paw edema by treatment with a neutrophil-depleting antibody (1A8). (**d**) Comparison of paw edema in *Ncf1*** and WT mice.

supernatants from low-density cultures (5×10^6 neutrophils ml^{-1}), their concentrations were substantially reduced in supernatants from high-density neutrophil cultures (10^8 cells ml^{-1}) (**Fig. 4a**). To analyze the whereabouts of neutrophil-derived cytokines and chemokines in high-density cultures, we isolated preformed aggNETs, washed and transferred them to fresh medium and then quantified their concentration in the medium. AggNETs contained substantial amounts of IL-8 and the anti-inflammatory IL-1 receptor antagonist (IL-1RA) but none of the other proinflammatory mediators analyzed (**Supplementary Fig. 7**). Attempts to liberate the inflammatory mediators by grinding and mechanical disruption of the aggregates or by heating in denaturing buffers failed to recover any neutrophil-derived cytokines and chemokines apart from IL-1RA and IL-8 (data not shown). These results excluded the possibility that the bulk of neutrophil-derived inflammatory mediators are merely trapped inside the aggNETs.

Next we incubated aggNETs with exogenous cytokines and chemokines and monitored their concentrations in the supernatants. Apart from IL-8, which is released in high amounts from aggNETs, we observed a time-dependent decrease in the concentration of cytokines and chemokines in the media containing aggNETs (**Fig. 4b**), which we did not observe in the absence of aggNETs (**Fig. 4b**). We also observed the degradation of inflammatory mediators with cell pellets of neutrophils from healthy subjects incubated with MSU, but this effect was strongly attenuated using neutrophils from subjects with CGD (**Supplementary Fig. 8**). The concentrations of IL-1β, the main proinflammatory cytokine released during acute gouty attacks, and its precursor protein were decreased in the presence of aggNETs (**Supplementary Fig. 9a**).

To examine the mechanism by which cytokines are degraded by aggNETs, we assessed whether they were trapped by transglutaminases
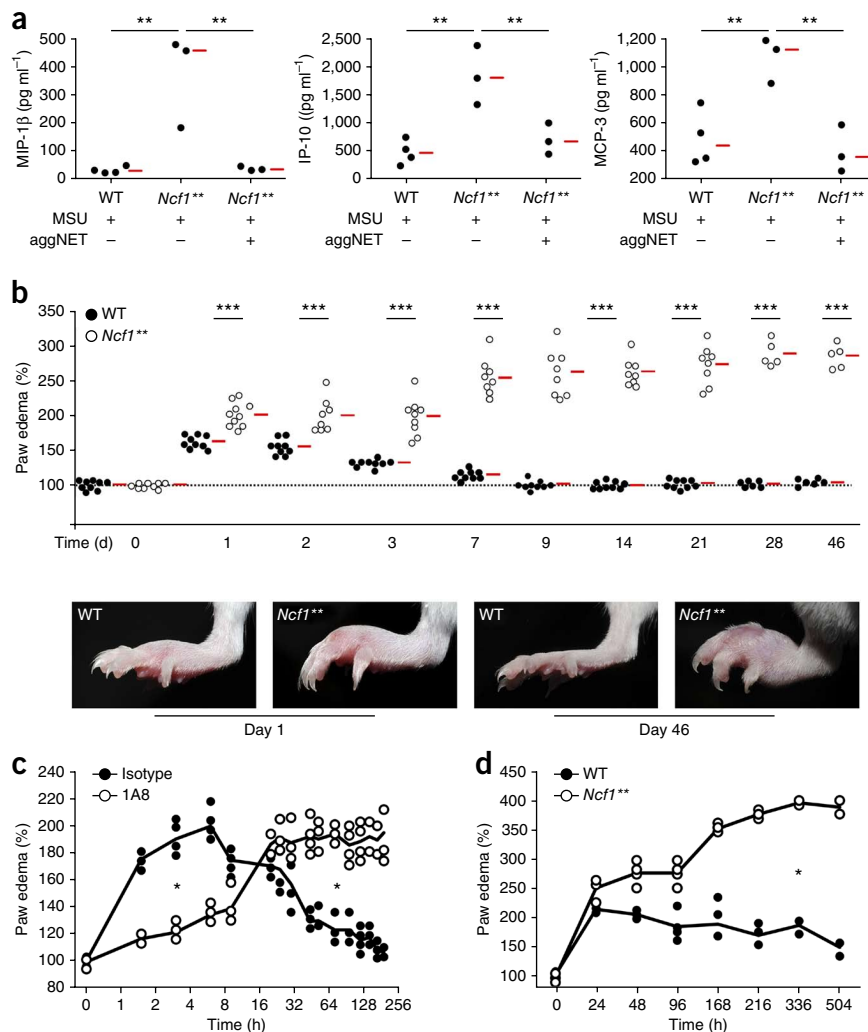
or proteolytically degraded by proteases. Treatment with EDTA or inhibitors of tissue transglutaminases did not prevent degradation of cytokines and chemokines by aggNETs (**Supplementary Fig. 9b**). However, blockade of proteinase 3 and elastase with elafin, suramin and sivelestat or incubation with the serine proteinase inhibitor PMSF inhibited inflammatory mediator degradation by aggNETs (**Fig. 4c** and **Supplementary Fig. 9c**).

Cell pellets from aggNETs generated by MSU incubation contain proteolytically active neutrophil elastase that is able to convert N-methoxysuccinyl-AAPV p-nitroanilide, a substrate of NE (**Fig. 4d**). However, cell pellets from neutrophils stimulated with the microbial peptide formyl-MLP (fMLP), which induces activation and degranulation of neutrophils without NETosis[17,26], or with DNA isolated from lysed neutrophils did not exhibit NE activity. Supernatants from fMLP- and, to a lesser extent, MSU-stimulated neutrophils exhibited NE activity. This result suggests that NETosis-inducing stimuli, such as MSU crystals, trigger NE activity that remains associated with the aggNET structure and is not just released into the supernatant during degranulation of neutrophils.

Impaired aggNET formation results in exacerbated and chronic inflammation

After MSU injection, we detected higher amounts of proinflammatory cytokines in lavages of air pouches in *Ncf1*** as compared to WT mice (**Supplementary Fig. 10**). We inferred that ROS-mediated

formation of aggNETs may degrade inflammatory mediators *in vivo*. Adoptive transfer of aggNETs into air pouches of *Ncf1*** mice reduced MSU-induced chemokine secretion to the values seen in WT mice (**Fig. 5a**).

We prevented aggregation of NETs by co-injecting DNase I with MSU crystals into air pouches of WT mice. DNase I reduced aggNET formation in WT mice (**Supplementary Fig. 11a**) and increased the concentrations of IP-10 and the mouse IL-8 homolog KC (**Supplementary Fig. 11b**).

To assess the pathogenic implications of these findings *in vivo*, we induced gout by subcutaneous injection of MSU crystals into the foot pads of WT and *Ncf1*** mice. In WT mice, injection of MSU crystals led to rapid but self-limited paw erythema and swelling. In contrast, in NETosis-deficient *Ncf1*** mice, paw edema was increased shortly (1 to 2 days) after MSU injection as compared to WT mice and exhibited a chronic course, with paw swelling that was apparent for several weeks after MSU injection (**Fig. 5b**) and higher concentrations of inflammatory mediators in the chronically inflamed paws (**Supplementary Fig. 12**). These results indicate that NETosis and the aggregation of NETs (tophus formation) promote resolution of MSU-induced inflammation in gout.

To examine whether similar mechanisms dampen neutrophilic inflammation in other models, we induced paw inflammation by injection of the yeast cell-wall polysaccharide zymosan. Zymosan induces NETosis (**Supplementary Fig. 4**) and activates TLR2, a receptor that in mice is expressed on neutrophils but also macrophages and lymphocytes. To ensure that zymosan-induced inflammation in the mouse is driven by neutrophils, we compared the disease course in neutrophil-depleted and isotype-treated mice (**Fig. 5c**). In isotype-treated mice, paw edema increased until 6 h of exposure to zymosan but decreased afterwards. In neutrophil-depleted mice, early paw edema was delayed but increased to isotype-treated levels at later time points and persisted. Zymosan-induced arthritis was also stronger and exhibited a chronic disease course in *Ncf1*** as compared to WT mice (**Fig. 5d**). These results suggest that neutrophils and NETosis promote the resolution of neutrophilic inflammation in conditions other than gout.

DISCUSSION

The clearance of neutrophils by mononuclear phagocytes is important for the resolution of inflammation in tissues with high amounts of infiltrating leukocytes[27]. Here our results suggest that inflammation can be attenuated by the action of aggregated NET structures formed under conditions of high neutrophil density. These MSU crystal–triggered aggNETs trap and proteolytically degrade neutrophil-derived cytokines and chemokines, reducing inflammation. This mechanism (**Supplementary Fig. 13**) may account for the enigmatic spontaneous remission of acute inflammatory attacks elicited by MSU crystals in individuals with gout and may be of importance to other forms of neutrophilic inflammation as well.

In agreement with published data, we observed that MSU-induced NETosis was preceded by the production of ROS[5,28] and resulted in the release of proinflammatory mediators from neutrophils cultured in densities comparable to those in the early phase of neutrophil recruitment or in the peripheral blood[29,30]. In contrast, higher densities of neutrophils, as occur in the synovial fluid of gouty arthritis or densely infiltrated inflammatory tissues[22], formed aggNETs *in vitro* and *in vivo*. These aggNETs shared characteristics with gouty tophi, including extended areas of extracellular DNA that are decorated with material from neutrophil granules and interspersed with MSU crystals[19,31].

MSU crystal–induced aggNET formation was augmented by ATP and lactoferrin, a specific inhibitor of neutrophil migration[32]. The release of ATP during NET formation is of importance, as extracellular nucleotides initiate clearance of dead cells by mononuclear phagocytes[33]. Both ATP and lactoferrin have an additional function in NET aggregation: in low-density cultures, the local concentrations of the short-lived ATP and of lactoferrin are below the threshold required for NET aggregation. Indeed, addition of both mediators also promoted aggNET formation in low density cultures.

Aggregation of NETs induced degradation of inflammatory mediators released by activated neutrophils and terminated the inflammatory response. This finding is consistent with the clinical observation that tophi in patients with chronic gout are frequently found without any signs of inflammation[31]. Specific protease inhibitors prevented cytokine degradation. Serine proteases are bound to NETs but can also be released from activated neutrophils during degranulation[34]. By comparing inducers of NETosis and aggNET formation to the degranulating agent fMLP, we found that degradation of cytokines was mediated primarily by NET-associated proteolytic activity. In line with that finding, cell pellets from normal healthy donors but not from subjects with CGD were able to degrade inflammatory mediators.

Production of ROS during the oxidative burst has been associated with the promotion of inflammation and tissue damage, but in recent years, it has also been implicated in the regulation of inflammation and protection from autoimmunity[24,35–37]. Using mice that are unable to mount an oxidative burst in phagocytes, we show that lack of ROS results in an exacerbated and chronic course of MSU-triggered joint inflammation, suggesting that ROS production promotes termination of inflammation elicited by MSU. The anti-inflammatory effects of ROS could be mediated by the trapping and degradation of cytokines in aggNETs. Two types of myeloid phagocytes, neutrophils and monocytes/macrophages, reportedly respond to MSU crystals. Whereas mononuclear phagocytes ingest the crystals and consecutively activate the NALP3 inflammasome[11], polymorphonuclear cells undergo proinflammatory NETosis or anti-inflammatory aggNET formation at low or high cell densities, respectively. Crosstalk between these pathways has to be considered, as IL-1β is implicated in NETosis potentially by autophagy[29], and aggNETs are able to degrade IL-1β. After MSU crystal–induced NETosis, recruitment of neutrophils may proceed until a threshold concentration of neutrophils is reached at the site of inflammation and aggNETs form. AggNETs then interrupt the inflammatory circle by degrading chemokines and proinflammatory cytokines such as IL-1β, thus bringing NETosis to a halt and resolving inflammation.

Therapeutic intervention exploiting the mechanisms described in this manuscript might involve shifting the balance toward the resolution of inflammation by promoting aggregation of NETs. Inducing aggNETs under conditions of functional NETosis would involve increasing the number of neutrophils by inhibiting cell migration. How this can be accomplished will be the subject of future studies.

METHODS

Methods and any associated references are available in the online version of the paper.

Note: Any Supplementary Information and Source Data files are available in the online version of the paper.

AUTHOR CONTRIBUTIONS

C.S. planned and performed most of the *in vitro* and *in vivo* experiments, conducted data analysis and wrote the manuscript. C.J., L.E.M., B.F., Y.Z., D.K., I.J. and R.B. performed *in vivo* and *in vitro* experiments and conducted data analyses. R.H. provided the *Ncf1**** mice and discussed the strategy of the experiments. M.L., B.M. and J.R. arranged and conducted the DECT analyses. E.N. performed and evaluated immune histology. T.H. and V.K. contributed samples from patients with CGD or gout and controls and provided scientific input. B.M., R.H., L.E.M. and G.S. provided scientific input and wrote the manuscript. Markus Hoffmann planned the experiments, provided scientific input and wrote the manuscript. Martin Herrmann supervised the project, planned and conducted experiments and data analysis and wrote the manuscript. All authors read and approved the manuscript.

COMPETING FINANCIAL INTERESTS

The authors declare no competing financial interests.

Reprints and permissions information is available online at http://www.nature.com/reprints/index.html.

1. Brinkmann, V. *et al.* Neutrophil extracellular traps kill bacteria. *Science* **303**, 1532–1535 (2004).
2. Urban, C.F., Reichard, U., Brinkmann, V. & Zychlinsky, A. Neutrophil extracellular traps capture and kill *Candida albicans* yeast and hyphal forms. *Cell. Microbiol.* **8**, 668–676 (2006).
3. Yipp, B.G. *et al.* Infection-induced NETosis is a dynamic process involving neutrophil multitasking *in vivo. Nat. Med.* **18**, 1386–1393 (2012).
4. Fuchs, T.A. *et al.* Novel cell death program leads to neutrophil extracellular traps. *J. Cell Biol.* **176**, 231–241 (2007).
5. Schorn, C. *et al.* Bonding the foe—NETting neutrophils immobilize the pro-inflammatory monosodium urate crystals. *Front. Immunol.* **3**, 376 (2012).
6. Akong-Moore, K., Chow, O.A., von Kockritz-Blickwede, M. & Nizet, V. Influences of chloride and hypochlorite on neutrophil extracellular trap formation. *PLoS ONE* **7**, e42984 (2012).
7. Papayannopoulos, V., Metzler, K.D., Hakkim, A. & Zychlinsky, A. Neutrophil elastase and myeloperoxidase regulate the formation of neutrophil extracellular traps. *J. Cell Biol.* **191**, 677–691 (2010).
8. Wu, X.W., Lee, C.C., Muzny, D.M. & Caskey, C.T. Urate oxidase: primary structure and evolutionary implications. *Proc. Natl. Acad. Sci. USA* **86**, 9412–9416 (1989).
9. Shi, Y., Evans, J.E. & Rock, K.L. Molecular identification of a danger signal that alerts the immune system to dying cells. *Nature* **425**, 516–521 (2003).
10. So, A. Neue erkenntnisse zur pathophysiologie und therapie der gicht. *Z. Rheumatol.* **66**, 562–567 (2007).
11. Martinon, F., Petrilli, V., Mayor, A., Tardivel, A. & Tschopp, J. Gout-associated uric acid crystals activate the NALP3 inflammasome. *Nature* **440**, 237–241 (2006).
12. Schorn, C. *et al.* Sodium overload and water influx activate the NALP3 inflammasome. *J. Biol. Chem.* **286**, 35–41 (2011).
13. Kasama, T. *et al.* Neutrophil-derived cytokines: potential therapeutic targets in inflammation. *Curr. Drug Targets Inflamm. Allergy* **4**, 273–279 (2005).
14. Ryckman, C. *et al.* Monosodium urate monohydrate crystals induce the release of the proinflammatory protein S100A8/A9 from neutrophils. *J. Leukoc. Biol.* **76**, 433–440 (2004).
15. Schorn, C. *et al.* The uptake by blood-borne phagocytes of monosodium urate is dependent on heat-labile serum factor(s) and divalent cations. *Autoimmunity* **43**, 236–238 (2010).
16. Scanu, A. *et al.* Cytokine levels in human synovial fluid during the different stages of acute gout: role of transforming growth factor β1 in the resolution phase. *Ann. Rheum. Dis.* **71**, 621–624 (2012).
17. Urban, C.F. *et al.* Neutrophil extracellular traps contain calprotectin, a cytosolic protein complex involved in host defense against *Candida albicans. PLoS Pathog.* **5**, e1000639 (2009).
18. Choi, H.K. *et al.* Dual energy computed tomography in tophaceous gout. *Ann. Rheum. Dis.* **68**, 1609–1612 (2009).
19. Manger, B., Lell, M., Wacker, J., Schett, G. & Rech, J. Detection of periarticular urate deposits with dual energy CT in patients with acute gouty arthritis. *Ann. Rheum. Dis.* **71**, 470–472 (2012).
20. Hakkim, A. *et al.* Activation of the Raf-MEK-ERK pathway is required for neutrophil extracellular trap formation. *Nat. Chem. Biol.* **7**, 75–77 (2011).
21. Brinkmann, V. & Zychlinsky, A. Beneficial suicide: why neutrophils die to make NETs. *Nat. Rev. Microbiol.* **5**, 577–582 (2007).
22. Shah, K., Spear, J., Nathanson, L.A., McCauley, J. & Edlow, J.A. Does the presence of crystal arthritis rule out septic arthritis? *J. Emerg. Med.* **32**, 23–26 (2007).
23. Beyer, C. & Pisetsky, D.S. Modeling nuclear molecule release during *in vitro* cell death. *Autoimmunity* **46**, 298–301 (2013).
24. Hultqvist, M. *et al.* Enhanced autoimmunity, arthritis, and encephalomyelitis in mice with a reduced oxidative burst due to a mutation in the Ncf1 gene. *Proc. Natl. Acad. Sci. USA* **101**, 12646–12651 (2004).
25. Sareila, O., Jaakkola, N., Olofsson, P., Kelkka, T. & Holmdahl, R. Identification of a region in p47phox/NCF1 crucial for phagocytic NADPH oxidase (NOX2) activation. *J. Leukoc. Biol.* **93**, 427–435 (2013).
26. Remijsen, Q. *et al.* Neutrophil extracellular trap cell death requires both autophagy and superoxide generation. *Cell Res.* **21**, 290–304 (2011).
27. Savill, J., Dransfield, I., Gregory, C. & Haslett, C. A blast from the past: clearance of apoptotic cells regulates immune responses. *Nat. Rev. Immunol.* **2**, 965–975 (2002).
28. Papayannopoulos, V. & Zychlinsky, A. NETs: a new strategy for using old weapons. *Trends Immunol.* **30**, 513–521 (2009).
29. Mitroulis, I. *et al.* Neutrophil extracellular trap formation is associated with IL-1β and autophagy-related signaling in gout. *PLoS ONE* **6**, e29318 (2011).
30. Keshari, R.S. *et al.* Neutrophil extracellular traps contain mitochondrial as well as nuclear DNA and exhibit inflammatory potential. *Cytometry A* **81**, 238–247 (2012).
31. Pascual, E., Batlle-Gualda, E., Martinez, A., Rosas, J. & Vela, P. Synovial fluid analysis for diagnosis of intercritical gout. *Ann. Intern. Med.* **131**, 756–759 (1999).
32. Bournazou, I. *et al.* Apoptotic human cells inhibit migration of granulocytes via release of lactoferrin. *J. Clin. Invest.* **119**, 20–32 (2009).
33. Elliott, M.R. *et al.* Nucleotides released by apoptotic cells act as a find-me signal to promote phagocytic clearance. *Nature* **461**, 282–286 (2009).
34. Gresnigt, M.S. *et al.* Neutrophil-mediated inhibition of proinflammatory cytokine responses. *J. Immunol.* **189**, 4806–4815 (2012).
35. Olofsson, P. *et al.* Positional identification of Ncf1 as a gene that regulates arthritis severity in rats. *Nat. Genet.* **33**, 25–32 (2003).
36. Campbell, A.M., Kashgarian, M. & Shlomchik, M.J. NADPH oxidase inhibits the pathogenesis of systemic lupus erythematosus. *Sci. Transl. Med.* **4**, 157ra141 (2012).
37. Jacob, C.O. *et al.* Lupus-associated causal mutation in neutrophil cytosolic factor 2 (NCF2) brings unique insights to the structure and function of NADPH oxidase. *Proc. Natl. Acad. Sci. USA* **109**, E59–E67 (2012).

ONLINE METHODS

Preparation of human material. All analyses of human material were performed in full agreement with institutional guidelines and with the approval of the Ethical committee of the University Hospital Erlangen (permit # 193_13B). Informed consent and permission to publish patient photos were obtained from all subjects enrolled in the study.

We extracted autologous plasma for culture from heparinized (20 U ml^{-1}) venous blood from NHDs by centrifugation at 3,900g for 10 min. Neutrophils and peripheral blood mononuclear cells (PBMCs) were isolated from heparinized blood of NHDs and patients with CGD by routine Ficoll density gradient centrifugation using standard protocols[38]. Briefly, we collected PBMCs and neutrophils from buffy coats, removed remaining platelets by centrifugation through a cushion of FBS (Invitrogen) and eliminated residual erythrocytes by hypotonic lysis. Viable cells were counted by trypan blue exclusion in a Neubauer chamber. We prepared paraffin sections of tophi and control tissue from subjects with gout and MSU-free synovitis. Synovial fluids were obtained from subjects with gout and with MSU-free synovitis by articular puncture.

Mice. *Ncf1*** mice, characterized by a point mutation in *Ncf1* (refs. 25,39), originate from The Jackson Laboratories and were backcrossed over more than ten generations to the BALB/c background and maintained at the animal facilities of the Universities of Erlangen or Lviv, respectively. The animal studies were approved by the local ethical committees and conducted according to the guidelines of the Federation of European Laboratory Animal Science Associations (FELASA). Genotyping of *Ncf1*** and WT littermates was done by pyrosequencing as described[24]. We obtained BALB/c and C57BL/6 mice from Charles River. All experiments were performed using age- and sex-matched littermate controls. Estimated necessary sample sizes were biometrically determined. Mice were allocated randomly into groups for neutrophil depletion and adoptive transfer experiments by a computer-based random number generator (http://www.randomizer.org) so that each cage contained animals of every group to compensate for possible cage effects.

DECT. We performed DECT scans during routine assessment in the outpatient clinic with a second-generation 128-slice dual-source CT system (Definition Flash, Siemens Healthcare) as described[19]. The data sets obtained were analyzed using a three-dimensional material decomposition algorithm allowing color-coded visualization and differentiation of MSU (green) from calcium (purple or gray).

Preparation of MSU crystals. For the production of MSU crystals, we adjusted a solution of 10 mM uric acid and 154 mM NaCl (both from Merck KGaA) to pH 7.2 and agitated it for 3 d. We washed the resulting crystals with ethanol, dried them under sterile conditions, sterilized them at 180 °C for 2 h and stored them in PBS (pH 7.0).

Analysis of NETosis and aggNET formation in neutrophils from NHDs, subjects with CGD and mice *in vitro*. We isolated neutrophils from NHDs or individuals with CGD and cultured them at 1×10^8 cells ml^{-1}, 2×10^7 cells ml^{-1} or 5×10^6 cells ml^{-1} with 20 pg per cell MSU crystals or zymosan (Invitrogen) for 1 h at 37 °C. NETosis and the formation of aggNETs were stopped by adding 1% paraformaldehyde to cell cultures. We analyzed aggNET formation in the presence or absence of the following inhibitors and agonists: 5 mM EDTA; 100 μg ml^{-1} DNase I (Roche); 300 μM oxATP, an antagonist of ATP; 100 μM Y-27632, an inhibitor of Rho kinase[40]; 10 μM ATP; 10–100 μM lactoferrin, 0.5 mM NAC, 10 μM DPI, 200 μM BHA and 300 μM ascorbic acid (all from Sigma-Aldrich); and 10–100 μM BSA (Merck KGaA). The size of the tophus/aggNET generated *in vitro* was determined by polarization and conventional light microscopy or on pictures made with a Nikon D800 reflex camera. Aggregation indices were calculated for each condition as the area of the largest coherent aggregate normalized to the mean area of the largest aggregate formed at high cell densities without inhibitors.

For whole-blood analyses in mice, we incubated heparinized whole blood (20 U ml^{-1}) with 1 mg ml^{-1} MSU crystals, zymosan or PBS for 2 h at 37 °C and prepared cytospins after removing erythrocytes by hypotonic lysis. We stained the nuclear and extranuclear DNA of the samples with 1 μg ml^{-1}

DAPI (Invitrogen) for 30 min. After washing, we analyzed the samples by fluorescence microscopy using standard filter sets.

For analysis of NETosis in human arthritides, we anticoagulated synovial fluids with 20 U ml^{-1} heparin, transferred the cells to glass slides by cytospin, stained them with DAPI and an antibody to NE (Abcam) and analyzed them by fluorescence microscopy.

Cytospin centrifugation. We centrifuged 2×10^5 cultured neutrophils at 960g for 10 min with a cytospin cuvette on glass slides (ThermoFisher). After removing the supernatants, the cells were centrifuged for 2 min at 2,500g. The fixed cells were analyzed by light and fluorescence microscopy.

Histology, immunohistochemistry and evaluation. We stained DNA in NETs with DAPI (Invitrogen), Hoechst 33342 (Molecular Probes, Eugene, USA) or PI (Invitrogen) at 1, 4 or 10 μg ml^{-1}, respectively, for 30 min. For the detection of NETs, we blocked fixed cells or sections with 10% BSA for 1 h. Samples were stained with antibodies to NE (1:200, Abcam, ab21595), myeloperoxidase (MPO; 1:200, Abcam, ab25989), CRAMP (1:100, Innovagen, PA-CRPL-100) or LL-37 (1:500, Hycult biotech, HM2070) in 10% BSA overnight at 4 °C. Secondary goat anti-rabbit or gout anti-mouse IgG antibodies conjugated with AlexaFluor 488 (SouthernBiotech) in blocking buffer were added and incubated for 2 h in the dark. The samples were analyzed by fluorescence microscopy using standard filter sets. Controls were stained with secondary antibody only.

***In vivo* generation and analysis of mouse aggNETs.** We pre-treated C57BL/6 mice with 2 ml of 2% thioglycolate (Sigma-Aldrich) solution by i.p. injection. Four days later, 20 mg MSU crystals were injected i.p. We analyzed the newly formed aggNETs (tophi) by DECT. Subsequently, aggNETs were harvested, and paraffin sections were prepared for analysis.

Liberation of proteins from aggNETs. AggNETs formed from 50 Mio neutrophils were weighed, submersed in 100 μl PBS and disrupted in tubes with steel beads on a Precellys Tissue Homogenizer (Peqlab). Alternatively, aggNETs were heated to 56 °C for 30 min in denaturing RIPA buffer containing Tris-HCl, pH 7.6, NP-40, sodium deoxycholate and SDS. After centrifugation of the disrupted material at 20,000g, total protein and selected cytokines in the supernatants were quantified by bicinchoninic acid (BCA) assay (Thermo Scientific) and bead assay, respectively. In BCA assays, protein concentrations ranged from 1.74 to 2.06 mg ml^{-1}.

Air pouch model and analyses of MSU- and zymosan-induced paw swelling in mice. We anesthetized mice with isofluorane and injected 3 ml of sterile air subcutaneously (s.c.) into the back to form an air pouch. Three days after the first injection, we injected an additional 2 ml of sterile air into the pre-existent pouch. Another 2 d later, we injected 5 mg MSU crystals in PBS, PBS only, 5 mg MSU plus 200 μg DNase I (Roche) or 200 μg DNase I alone into the air pouches. The pouch fluid was harvested at the time points indicated in the figures, and cytokine and chemokine levels were determined by multiplex bead technology (eBioscience) and quantified by cytofluorometry. The sizes of newly formed tophi in the air pouches were analyzed after surgical removal of the air pouch.

For the aggNET transfer experiments, we generated aggNETs by i.p. injection of 20 mg MSU crystals in mice pretreated with thioglycolate. 24 h later, we harvested aggNETs, washed them five times with PBS and transferred them to pregenerated air pouches.

For analysis of paw swelling, we injected 1.5 mg MSU or 300 μg zymosan (Invitrogen) in 70 μl PBS s.c. into the foot pads of WT and *Ncf1*** mice. As a control, we injected the contralateral foot pad with PBS. Paw swelling was measured with an electronic caliper by a blinded experimenter at the indicated time points. For depletion of neutrophils, mice were i.p. injected with 500 μg of Ly6G-specific antibody (clone 1A8, BioXCell) or isotype control antibody (clone 2A3, BioXCell) in PBS 40 h before zymosan application. The mice received a second injection of 500 μg 1A8/2A3 72 h after the first dose. The efficiency of neutrophil depletion was verified by flow cytometry and ranged between 90% and 95% depletion.

To determine the concentration of cytokines and chemokines in paws during MSU-induced arthritis, we homogenized mouse feet in protein extraction buffer

(20 mM 4-(2-hydroxyethyl)-1-piperazineethanesulfonic acid (HEPES), 0.4 mM NaCl, 1.5 mM MgCl$_2$, 5 mM β-mercaptoethanol, 1 mM EDTA, 1 mM ethylene glycol tetraacetic acid (EGTA) and 20% glycerol, pH 7.9) using the Precellys Steel Kit 2.8 mm on a tissue homogenizer (Peqlab). After sonication, samples were again homogenized and subsequently centrifuged (14,000 r.p.m., 15 min, 5 °C). Cytokine and chemokine levels of protein extracts were then analyzed by multiplex bead technology (eBioscience).

Inhibition of proteolytic activity of aggNETs and measurement of cytokines and chemokines. Neutrophils were incubated with MSU crystals (20 pg per cell) for 30, 120 or 360 min at 37 °C. Furthermore, externally added cytokines and chemokines (eBioscience) were incubated with aggNETs in 1% BSA for 0, 2, 6, 18 or 24 h. We used the following proteinase inhibitors: HALT cocktail mix (100 μM PMSF, 2 mM Na-orthovanadate, 10 mM NaF and 10 mM β-glycerophosphate; ThermoFisher); 1 μM elafin; 1 μM elafin plus 100 μM suramin, both of which are inhibitors of elastase and proteinase 3; 100 μg ml^{-1} sivelestat, an inhibitor of neutrophil elastase; 100 μM PMSF (all from Sigma-Aldrich); 10 μM z-DON (z-DON-Val-Pro-Leu-oMe, Zedira), an inhibitor of transglutaminase; or 5 mM EDTA[41–44]. Human cytokines and chemokines in culture supernatants were analyzed by multiplex bead technology (eBioscience) and quantified by cytofluorometry.

Analysis of neutrophil elastase activity. Isolated human neutrophils (1×10^8 cells ml^{-1}) were incubated with 5 mg MSU crystals or 1 μM of the bacteria-derived peptide fMLP for 2 h. Untreated neutrophils or total DNA isolated from human neutrophils using a Quick-gDNA kit (Zymo Research) were used as a control. We quantified NE activity in washed pellets and supernatants with 100 μM of the NE substrate N-methoxysuccinyl-Ala-Ala-Pro-Val 4-nitroanilide (Sigma-Aldrich). The release of p-nitroaniline was monitored at 405 nm on a Tecan Sunrise microplate reader (Tecan).

Measurement of human pro–IL-1β, IL-1β and calnexin levels in THP-1 lysates. We extracted total protein from THP-1 cells by hypotonic lysis of the cells. The expression of human pro–IL-1β and IL-1β was analyzed with a rabbit antibody to pro–IL-1β and IL-1β (1:1,000, Cell Signaling Technology, 2022S) by immunoblotting using standard protocols. Blots stained with Coomassie Blue served as loading controls.

Induction of necrosis in neutrophils. Primary necrosis was induced by treating freshly isolated neutrophils (1×10^6 ml^{-1}) with 10 μM melittin from honey bee venom for 30 min, 1 mM HgCl$_2$ for 60 min and 0.05% Triton X-100 for 60 min (all necrosis inducers; Sigma-Aldrich) or by heating at 70 °C for 5 min. Subsequently, cells were incubated for 30 min at 4 °C with 300 μl Ringer's solution (Delta Select) containing 1 μg ml^{-1} annexin A5–FITC (AxA5-FITC, Responsive GmbH) and 20 μg ml^{-1} PI (Sigma-Aldrich) and analyzed by flow cytometry. Necrosis induction was confirmed by changes in cellular morphology and AxA5-FITC and PI staining. The percentage of AxA5-FITC$^-$ and PI$^+$ (necrotic) cells was >95%.

Flow cytometry. We performed all flow cytometry analyses on a Gallios cytofluorometer (Beckman Coulter). The data were analyzed using Kaluza software (Beckman Coulter). We used electronic compensation to eliminate bleed-through fluorescence. The erythrocyte lysis conditions also solubilized non-ingested MSU crystals.

Morphometry and quantification of NETs and aggNETs. To detect changes in nuclear area, perimeter and shape that occur during NETosis and necrosis, we performed quantitative measurements using Adobe Photoshop CS5 Extended software on images from PI- or DAPI-stained cytospins or tissue sections or on photos from in vitro–generated aggNETs. We recorded the mean/maximum area of the nucleus/aggNET, circularity ($f_{circ} = 4^*\pi^*area/perimeter^2$) and intensity of the fluorescence signal.

Statistical analyses. Results are represented as the mean ± s.e.m. of at least three and up to eight independent experiments or the mean ± s.d. within a representative experiment. We performed computations and charts with SPSS PASW statistics 18 and GraphPad Prism 5.03 software. For calculation of statistical differences, we used Student's t test, Kruskal-Wallis test or Mann-Whitney U test with Dunnett's post-hoc test, where applicable. Adjusted $P < 0.05$ were considered to be statistically significant.

38. Nilsson, C. *et al.* Optimal blood mononuclear cell isolation procedures for γ interferon enzyme-linked immunospot testing of healthy Swedish and Tanzanian subjects. *Clin. Vaccine Immunol.* **15**, 585–589 (2008).
39. Huang, C.K., Zhan, L., Hannigan, M.O., Ai, Y. & Leto, T.L. P47(phox)-deficient NADPH oxidase defect in neutrophils of diabetic mouse strains, C57BL/6J-m db/db and db/+. *J. Leukoc. Biol.* **67**, 210–215 (2000).
40. Cinel, I. *et al.* Involvement of Rho kinase (ROCK) in sepsis-induced acute lung injury. *J. Thorac. Dis.* **4**, 30–39 (2012).
41. Cadène, M. *et al.* Inhibition of neutrophil serine proteinases by suramin. *J. Biol. Chem.* **272**, 9950–9955 (1997).
42. Iwata, K. *et al.* Effect of neutrophil elastase inhibitor (sivelestat sodium) in the treatment of acute lung injury (ALI) and acute respiratory distress syndrome (ARDS): a systematic review and meta-analysis. *Intern. Med.* **49**, 2423–2432 (2010).
43. Schaertl, S. *et al.* A profiling platform for the characterization of transglutaminase 2 (TG2) inhibitors. *J. Biomol. Screen.* **15**, 478–487 (2010).
44. Wiedow, O., Schroder, J.M., Gregory, H., Young, J.A. & Christophers, E. Elafin: an elastase-specific inhibitor of human skin. Purification, characterization, and complete amino acid sequence. *J. Biol. Chem.* **265**, 14791–14795 (1990).